

## Research Article

# Cardiac Imaging Using Clinical 1.5 T MRI Scanners in a Murine Ischemia/Reperfusion Model

Jakob G. J. Voelkl,<sup>1</sup> Bernhard J. Haubner,<sup>1</sup> Christian Kremser,<sup>2</sup> Agnes Mayr,<sup>2</sup>  
Gert Klug,<sup>1</sup> Alexander Loizides,<sup>2</sup> Silvana Müller,<sup>1</sup> Otmar Pachinger,<sup>1</sup> Michael Schocke,<sup>2</sup>  
and Bernhard Metzler<sup>1</sup>

<sup>1</sup>Department of Internal Medicine III (Cardiology), Innsbruck Medical University, Anichstr. 35, 6020 Innsbruck, Austria

<sup>2</sup>Department of Radiology I, Innsbruck Medical University, Anichstr. 35, 6020 Innsbruck, Austria

Correspondence should be addressed to Bernhard Metzler, bernhard.metzler@uki.at

Received 13 July 2010; Accepted 26 October 2010

Academic Editor: Andrea Vecchione

Copyright © 2011 Jakob G. J. Voelkl et al. This is an open access article distributed under the Creative Commons Attribution License, which permits unrestricted use, distribution, and reproduction in any medium, provided the original work is properly cited.

To perform cardiac imaging in mice without having to invest in expensive dedicated equipment, we adapted a clinical 1.5 Tesla (T) magnetic resonance imaging (MRI) scanner for use in a murine ischemia/reperfusion model. Phase-sensitive inversion recovery (PSIR) sequence facilitated the determination of infarct sizes *in vivo* by late gadolinium enhancement. Results were compared to histological infarct areas in mice after ischemia/reperfusion procedure with a good correlation ( $r = 0.807$ ,  $P < .001$ ). In addition, fractional area change (FAC) was assessed with single slice cine MRI and was matched to infarct size ( $r = -0.837$ ) and fractional shortening (FS) measured with echocardiography ( $r = 0.860$ ); both  $P < .001$ . Here, we demonstrate the use of clinical 1.5 MRI scanners as a feasible method for basic phenotyping in mice. These widely available scanners are capable of investigating *in vivo* infarct dimensions as well as assessment of cardiac functional parameters in mice with reasonable throughput.

## 1. Background

In cardiovascular research, the use of mouse models is gaining importance, based on the widespread utilization of genetically altered mice [1] and different disease models [2]. Due to small heart size and high heart rate, most cardiac imaging methods in mice have the disadvantage of requiring specialized and expensive equipment. Therefore, clinical echocardiography systems are the most frequently used investigative tool [3] in murine cardiac imaging, since dedicated animal echocardiography machines are not available in most institutions.

Recently, cardiac magnetic resonance imaging (CMR) has developed into a highly demanded imaging method in mice, because it provides measurements of a range of different parameters [4]. Many experiments have been conducted with specialized high-field (4.7 Tesla (T) to 17.6 T) magnetic resonance imaging (MRI) scanners, demonstrating them to be a valuable imaging method for cardiovascular

research [5–9]. However, these devices specialized for small animal imaging, are expensive and not accessible to most researchers. Although few experiments on mice have been conducted using standard 1.5 T MRI [10–13], hardware and imaging techniques have advanced in the meanwhile.

We sought to develop an easily accessible but versatile and accurate cardiac imaging method with adequate throughput for an ischemia/reperfusion (I/R) model [14] in mice by adapting a widely available 1.5 T MRI scanner with standard equipment provided by the manufacturer. The purpose of this study was to determine whether (a) it is possible to use late enhancement sequences [15] to detect myocardial infarction in the mouse heart at 1.5 T, (b) this method can detect differences in infarct size and whether results correlate with histological infarct size and (c) 1.5 T scanners can provide measurements of functional parameters to characterize the normal and impaired mouse heart.

Here, we evaluate the feasibility of standard 1.5 T MRI to determine infarct size *in vivo*. Additionally, we tested

the acquisition of quickly obtainable MRI-derived functional measurements to characterize heart function.

## 2. Methods

**2.1. Mouse Ischemia/Reperfusion Model.** Our investigation was carried out in two study groups. The first group comprising a total of 25 C57BL/6 mice, 12–15 weeks old, were randomized into subgroups of 0 min = sham ( $n = 6$ ), 30 min ( $n = 10$ ) and 60 min of ischemia ( $n = 9$ ) resulting in different infarction size. Mice underwent a well-established *in vivo* procedure of reversible LAD ligation as previously described [16–18] followed by 1 week of reperfusion. Briefly, following anesthesia, ventilation, and thoracotomy, the LAD was reversibly ligated aided by a PE tube. After the defined duration of ischemia, the PE tube was removed and reperfusion was visually confirmed. Three hours after reperfusion, troponin T was evaluated using a quantitative assay (Roche Diagnostics, Austria); 1 week after reperfusion, imaging procedures were performed and mice were sacrificed and the hearts excised for histological evaluation of infarct size. In a second study group ( $n = 18$ ) similar to the first one (sham:  $n = 6$ , 30 min:  $n = 6$  and 60 min:  $n = 6$ ), images were acquired and hearts were excised for histological evaluation of infarct size. Photoshop (Adobe, United States) software was used to create artwork. CMR images were enlarged to fit format. Animals were obtained from Charles River Laboratories and handled in accordance with institutional guidelines; all experiments were approved by the Institutional Ethics Committee and in accordance with the Guide for the Care and Use of Laboratory Animals published by the US National Institutes of Health (NIH Publication No. 85-23, revised 1996).

**2.2. Histology.** Hearts from the first study group were excised for histological evaluation after 1 week of reperfusion. Three 5- $\mu$ m sections were cut in 1 mm distance from the apex to the mid-section of the left ventricle for standard hematoxylin-eosin and Masson trichrome staining to detect collagen deposition and scar size. Slices were digitized with Axiom II (Zeiss, Germany), and infarct size was analyzed with Image J software from trichrome stainings [19].

Hearts from the second study group were excised after 24 h of reperfusion for triphenyl tetrazolium chloride (TTC) staining. TTC staining was performed to assess myocardial viability before scar formation. Whereas brick red areas indicate viable myocardium, white regions demarcate tissue injury. Hearts were cut in 1 mm thick slices which were digitized and analyzed with Image J software. Different staining protocols for the two groups were required due to different reperfusion times to permit infarct evaluation [6]. Infarct size was calculated in percentage of left ventricular myocardial area.

**2.3. MRI Image Acquisition.** Measurements were performed using a 1.5 T routine whole body MR scanner (Magnetom Avanto, Siemens, Germany) equipped with a 40 mT/m gradient system. In the first study group, MRI examinations

were performed before I/R procedure, 24 h and 1 week after procedure. In the second study group, late enhancement imaging was performed 24 h after procedure. Because of the essential noncardiodepressive characteristics of the widely used 222-tribromoethanol [20, 21], this sedative was used in this experiment, despite the known possible side effects [20, 22–24]. None of the mice showed any sign of the described side effects after intraperitoneal administration of 250 mg/kg 222-tribromoethanol at a dilution of 12.5 mg/ml. After sedation and injection of contrast agent, mice were placed prone inside a small loop coil (standard finger coil) with an inner diameter of 30 mm (see Supplementary Material available online at doi:10.1155/2011/185683). Mean heart rate during examinations was  $410 \pm 70$  beats per minute (bpm). For electrocardiography (ECG) gating, the standard equipment as provided by the MRI manufacturer was used: Siemens wireless peripheral monitoring unit attached to paws with trimmed Skintact conductor pads for children. Localizing protocols were performed, followed by functional measurements, and imaging was completed by acquisition of late enhancement sequences. Total acquisition time was approximately 20 min. Images were analyzed using JVision software (Agfa, Germany).

**2.4. Cine MRI.** After using localizers to determine heart axis (See supplemental file 2), a short-axis single slice cine imaging was performed at papillary muscle level of the heart, mirroring echocardiographic imaging procedure, followed by a long-axis scan (See supplemental files 3, 4 and 5). For cine imaging (Figure 2), a 2D-FLASH sequence was used (repetition time (TR) = 13 ms, echo time (TE) = 6.2 ms, flip angle: 15°, number of slices: 1, slice thickness: 2 mm, number of excitations: 4; field of view: 90 mm  $\times$  62 mm and an acquisition matrix of 256  $\times$  141). An average of 12 cardiac phases was acquired (acquisition time was about 3 min), and fractional area change (FAC) and fractional shortening (FS) were determined from these images. Thereafter, a short-axis cine imaging (number of excitations: 1; slice thickness: 1.5 mm) with 3-4 subsequent slice positions covering the whole left ventricle was performed for calculation of ejection fraction. Ejection fraction was calculated with Siemens Argus software [25] (See supplementary material). FAC and FS (measured parallel and perpendicular to the septum) were calculated using the standard formula (FS:  $((LV$  enddiastolic diameter –  $LV$  endsystolic diameter)/ $LV$  enddiastolic diameter)  $\times$  100; FAC  $((LV$  enddiastolic area –  $LV$  endsystolic area)/ $LV$  enddiastolic area)  $\times$  100).

**2.5. Late Enhancement Imaging.** Gadolinium-DOTA was administered intravenously before imaging procedure. Best results were obtained when concentration of the contrast agent used was 0.6 mmol/kg and LGE measurements were conducted 20 min after administration at the end of the imaging routine [7, 26, 27].

After registering cine MRI sequences, a segmented 2D phase-sensitive inversion recovery trueFISP sequence (PSIR) [25, 26] (Figure 1) with the following parameters was used: TR = 328 ms; TE = 2.72 ms; flip angle: 45°; inversion time

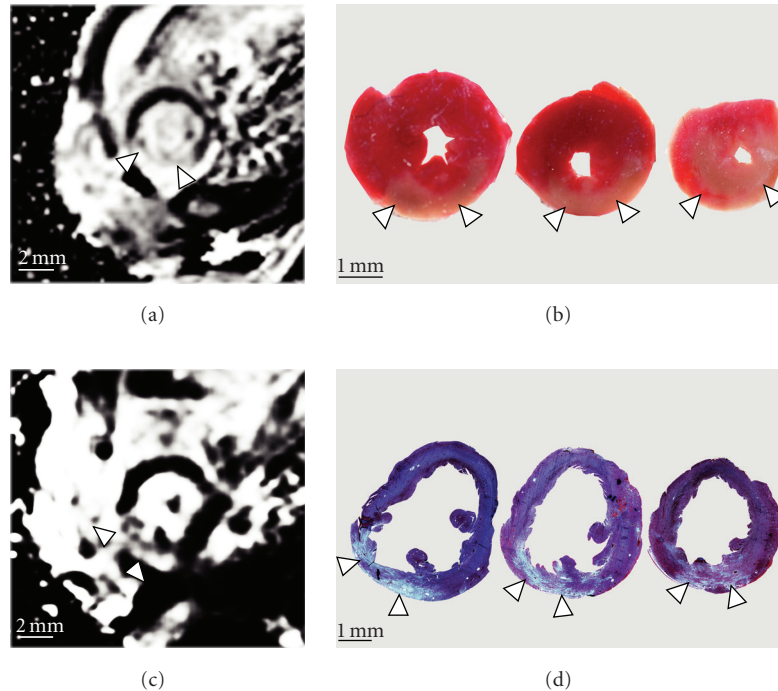


FIGURE 1: Myocardial infarction shown by LGE in magnetic resonance imaging and histological staining. Representative slices taken from the left ventricle: LGE shown by phase-sensitive inversion recovery trueFISP sequence (PSIR) (a) compared with 3 successive slices from the same heart after triphenyl tetrazolium chloride staining (b) 24 h after procedure. LGE shown by PSIR sequence (c) compared with 3 slices from the same heart after trichrome staining (d) 1 week after procedure. Arrows indicate area of infarction.

(TI) = 320 ms; slice thickness: 2.5 mm; field of view: 80 mm  $\times$  72 mm; acquisition matrix: 256  $\times$  168. The parameters were chosen such that data acquisition took place during the R-R interval in order to minimize artifacts caused by heart motion. The typical acquisition time was 60 seconds. Additionally, an ECG-gated 3D inversion recovery-prepared single shot gradient-echo sequence (turbo fast low angle shot, turboFLASH) was used covering the whole heart with a slice thickness of 0.8 mm (see supplemental file 7). Typical acquisition parameters were as follows: TR = 437 ms, TE = 5.78 ms, TI = 270 ms, flip angle: 15°, acquisition matrix: 384  $\times$  512, FOV: 56 mm  $\times$  75 mm. Fat saturation was used to suppress the fat signal.

**2.6. Echocardiography.** Echocardiographic examinations were performed 3 to 4 h after MRI imaging; mice were again sedated with 250 mg/kg 222-tribromoethanol. Myocardial contractility was determined by transthoracic echocardiography (See supplementary material), using a clinical echocardiography system (Acuson Sequoia C512, Acuson Corporation, United States) with Acuson15 L8 transducer (15 Mhz). FS was calculated from short-axis 2D-targeted M-mode images of the left ventricle [3]. Average heart rate during echocardiography was 518  $\pm$  60 bpm.

**2.7. Statistical Analysis of Data.** Statistical tests were performed with SPSS 15.0 software. Data were analyzed using

one way ANOVA test followed by *post hoc* multiple comparison test; for correlation the Pearson correlation test was used. All data are expressed as mean  $\pm$  standard deviation. Probability values <.05 were considered significant.

### 3. Results

**3.1. Evaluation of Infarct Size.** Three mice were excluded from the study due to poor image quality and were not included in the numbers of mice in the study. In every mouse of the 30 and 60 min ischemia group, myocardial infarction was detected by CMR and histology. No infarction was found in sham mice. Furthermore, the 60-min ischemia group had significantly larger infarct sizes than the 30-min group determined by either CMR PSIR sequences or histology (Table 1). We found no significant difference of infarct size measured with CMR and histological methods.

In the first study group (1 week reperfusion), correlation of histological observers was  $r = 0.793$  and  $r = 0.807$ , both  $P < .001$  (Figure 3) demonstrating good interobserver agreement of  $r = 0.806$ ,  $P < .001$  (sham mice excluded). Troponin T values correlated reasonably well with infarct size (1W) determined by either CMR LGE ( $r = 0.684$ ,  $P = .007$ ) or histological staining ( $r = 0.628$ ,  $P = .016$ ); sham mice excluded.

Furthermore, the second study group (24 h reperfusion) revealed good correlation of LGE imaging with their

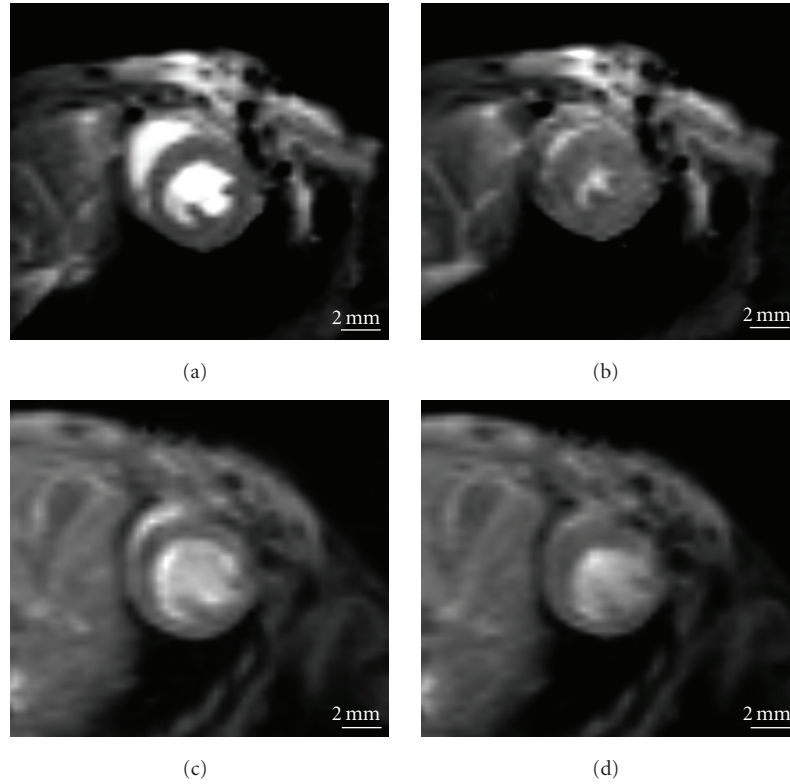


FIGURE 2: Short-axis cine magnetic resonance imaging of the mouse heart. Mouse heart in cardiac cine magnetic resonance imaging 1 week after sham operation ((a): diastolic, (b): systolic) and 60 min ischemia ((c): diastolic, (d): systolic).

TABLE 1: Infarct size in mouse heart after I/R procedure. Infarct size measured in magnetic resonance imaging by LGE in magnetic resonance imaging and histology (24 h after reperfusion by TTC staining and 1 week after reperfusion by trichrome staining). No infarction was detected in sham-operated mice. Values shown as mean percentage of left ventricular area  $\pm$  standard deviation. \*Significant difference to 30 min ischemia operated mice, all  $P < .05$ .

|   | 30 min         | 60 min           |
|---|----------------|------------------|
| Infarction area histology (TTC) 24 h (%)      | 17.7 $\pm$ 4.3 | 33.1 $\pm$ 7.1*  |
| Infarction area LGE 24 h (%)                  | 20.6 $\pm$ 7.8 | 37.1 $\pm$ 8.7*  |
| Infarction area histology (trichrome) 1 W (%) | 15.9 $\pm$ 7.7 | 35.6 $\pm$ 15.2* |
| Infarction area LGE 1 W (%)                   | 18.3 $\pm$ 4.4 | 38.3 $\pm$ 10.2* |

respective TTC stainings ( $r = 0.793$ ,  $P = .002$ ; sham mice excluded).

**3.2. Cardiac Functional Parameters.** Cardiac function (Table 2) determined by FAC measured in cine MRI correlated well with FS measured in echocardiography (correlation of all measurements: before procedure, 24 h and 1 week after procedure:  $r = 0.860$ ,  $P < .001$ ). A significant difference in cardiac function was found between the groups (Figure 3). Comparison of FS measured by CMR and echocardiography showed a correlation of  $r = 0.820$ ,

$P < .001$ ; correlation between FS and FAC measured by CMR was  $r = 0.863$ ,  $P < .001$ .

**3.3. Correlation of Infarct Size with Functional Parameters.** Correlation of histological infarct size 1 week after procedure with functional parameters was CMR-determined FAC  $r = -0.837$ , CMR-determined FS  $r = -0.768$  and echocardiography-determined FS  $r = -0.782$ ; all  $P < .001$ . Infarct size determined by LGE in MRI also showed good correlations with functional parameters: CMR-determined FAC  $r = -0.860$ , CMR-determined FS  $r = -0.758$ , and echocardiography-determined FS  $r = -0.845$ ; all  $P < .001$ . Troponin T levels correlated to functional measurements revealed similar results: Troponin T correlated to FAC (CMR):  $r = -0.781$ ,  $P < .001$ ; FS (CMR)  $r = -0.735$ ,  $P < .001$ ; FS (Echocardiography)  $r = -0.663$ ,  $P = .001$ .

## 4. Discussion

The following are the three major findings of this study. (a) It is possible to use late enhancement sequences to determine infarct size in mice with a clinical MRI scanner; (b) Infarct size measured with MRI shows good correlation with histological infarct size; (c) Functional parameters determined with cine MRI show good correlation with infarct size and standard echocardiography.

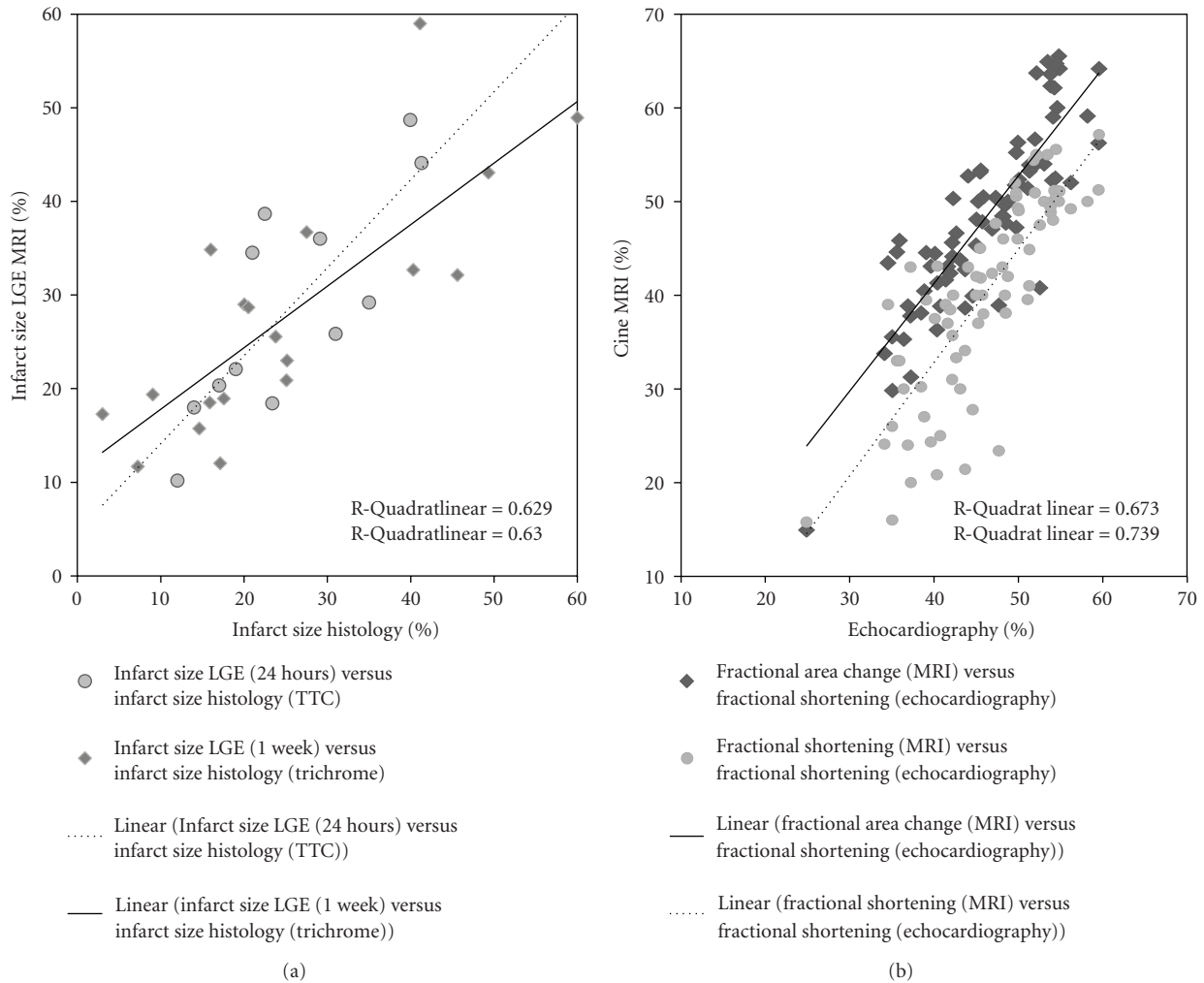


FIGURE 3: Regression plot showing infarct size and functional parameters. Regression plot of infarct size (a) measured in magnetic resonance imaging with LGE (Y axis) compared with histological infarct size in TTC staining (X axis) 24 h after procedure (a—circles, broken line). Infarct size determined by magnetic resonance imaging (Y axis) compared with histological infarct size in trichrome staining (X axis) 1 week after procedure (a—rhombi, continuous line). Regression plot of functional parameters (b): fractional area change (FAC) (b—rhombi, continuous line) and fractional shortening (FS) (b—circles, broken line) measured in cine magnetic resonance imaging (Y axis) compared with fractional shortening (FS) measured with echocardiography (X axis).

To ease access to murine cardiac imaging, we successfully adapted a clinical 1.5 T MRI scanner for *in vivo* phenotyping using a mouse ischemia/reperfusion model.

We first tested the use of late enhancement [15] sequences for *in vivo* infarct size quantification in C57Bl/6 mice after I/R procedure and validated it by comparing it with histological infarct size. Clinical scanners, however, lack the spatial and temporal resolution required for detailed imaging. This results in the lower correlation of our MRI LGE measurements and histology when compared with results from dedicated rodent scanners [27]. However, our results indicate that a good estimate of infarct size in mice *in vivo* is possible on a clinical scanner. The PSIR rather than a FLASH-3D sequence was chosen for evaluation of infarct size because of its relative resistance to motion artifacts, at the cost of higher slice thickness.

In agreement with other investigations [12, 13], there was a good correlation between the results of functional measurements by cine CMR and the established standard echocardiography in mice. The good correlation of impaired cardiac function with infarction size and the difference of cardiac function found between the different reperfusion groups highlight the capability of clinical MRI to detect functional differences between the normal and impaired mouse heart.

FS is the established parameter to characterize LV function in mice and, measured by MRI, shows good correlation to echocardiographic measurements of FS and infarct size. Due to localizing protocols, MRI permits easy standardization of imaging procedures allowing for more advanced techniques routinely used. Ejection fraction was already shown useful elsewhere [13] and similar results

were achieved in this study (See supplementary material). Since measurement of EF is time consuming and challenging on a 1.5 T MRI scanner, we investigated the use of FAC to describe cardiac function. FAC showed good correlation with infarct size that was even better than FS. This suggests that, while measurement of EF is the proper standard, single slice measurement of FAC can give a good estimate of myocardial function impaired by I/R injury, and at the same time, is a simple, robust, and fast imaging modality for routine use.

We were able to acquire these data without expensive specialized equipment. To our knowledge, this was not possible prior to the establishment of this imaging protocol. The ability of clinical MRI scanners to acquire versatile information, with good correlation to established methods, demonstrates its capacity to characterize the extent of myocardial infarction and cardiac functions in mice. Higher field strength MRI scanners are traditionally used in murine models, and clinical 1.5 T MRI scanners are of limited value in this area of research. An adapted clinical scanner obviously cannot perform as well as specialized rodent scanners [6, 27]. However, as our data indicate, this imaging method can provide a valuable imaging alternative for basic cardiac phenotyping. If imaging sequences are reduced to those discussed here (localizing sequences, followed by a short-axis cine sequence and PSIR sequence), image acquisition of the mouse heart can be accomplished in approximately 6-7 min.

Experiments conducted on 1.5 T MRI by other investigators used different settings for slice thickness and field of view, at the cost of temporal resolution, obtainable cardiac phases and therefore of image quality [12, 13]. The results from these studies already hinted at the potential of adapting clinical scanners. Advances in hardware and modified sequences enabled us to improve our settings for the representation of cardiac function while minimizing artifacts.

3T MRI scanners, available in future in an increasing number of institutions [11], can be adapted in the same manner as shown here and may provide even better imaging quality. However, this study was performed on a 1.5 T MRI to demonstrate the potential of clinical scanners.

In clinical MRI scanners, high heart rate in mice can cause motion artifacts in PSIR sequence when using segmentation factors >10 (typical patient examination: segmentation factor: 65 [25, 28]), mimicking LGE. To prevent this, ECG gating and MRI protocols should be optimized, images should be interpreted by trained observers and sedation should be adequate [29]. While a low heart rate is beneficial for LGE sequences, measurements of functional parameters require a heart rate close to physiological condition [30]. During MRI measurements, mean heart rate of the animals was lower than during echocardiographic measurements. This may be due to the different environment in the MRI scanner. Nonetheless, in the absence of dedicated animal echocardiography machines, a clinical MRI scanner employed in accordance with the protocol we present in this study, can provide valuable imaging data for basic cardiac phenotyping.

TABLE 2: Cardiac functional parameters. Fractional shortening (FS) determined by echocardiography and cine magnetic resonance imaging (MRI), fractional area change (FAC) determined by cine magnetic resonance imaging. Values shown as mean percentage  $\pm$  standard deviation before (preop), 24 h and 1 week after ischemia/reperfusion procedure for mice with no ischemia (sham), 30 min or 60 min of ischemia during procedure. Troponin T levels (ng/ml) are shown for each group. \*Significant difference to sham-operated mice; †Significant difference to 60 min operated mice; all  $P < .05$ .

|                    | 0 min = sham                | 30 min                       | 60 min           |
|--------------------|-----------------------------|------------------------------|------------------|
| FS echo preop (%)  | 50.8 $\pm$ 3.7              | 50.5 $\pm$ 3.1               | 51.5 $\pm$ 3.6   |
| FS MRI preop (%)   | 48.2 $\pm$ 5.1              | 47.5 $\pm$ 5.3               | 47.4 $\pm$ 3.6   |
| FAC preop (%)      | 55.5 $\pm$ 5.4              | 55.7 $\pm$ 6.3               | 52.5 $\pm$ 2.7   |
| FS echo 24 h (%)   | 51 $\pm$ 5.5 <sup>†</sup>   | 41.1 $\pm$ 5.6*              | 40.7 $\pm$ 3.6*  |
| FS MRI 24 h (%)    | 45.8 $\pm$ 8.6 <sup>†</sup> | 33.1 $\pm$ 9.7*              | 26.2 $\pm$ 4.6*  |
| FAC 24 h (%)       | 55.3 $\pm$ 6.9 <sup>†</sup> | 42.8 $\pm$ 6.9*              | 38.6 $\pm$ 3.6*  |
| FS echo 1 W (%)    | 55.3 $\pm$ 1.6 <sup>†</sup> | 43.2 $\pm$ 4.2* <sup>†</sup> | 37.7 $\pm$ 5.9*  |
| FS MRI 1 W (%)     | 50.7 $\pm$ 2.4 <sup>†</sup> | 39.1 $\pm$ 5.4* <sup>†</sup> | 32.2 $\pm$ 10.2* |
| FAC 1 W (%)        | 59.6 $\pm$ 6.1 <sup>†</sup> | 46.4 $\pm$ 2.8* <sup>†</sup> | 36.9 $\pm$ 8.8*  |
| Troponin T (ng/ml) | 0.1 $\pm$ 0.1               | 2.4 $\pm$ 0.7*               | 3.8 $\pm$ 2.0*   |

## 5. Conclusions

Mouse models are an important tool in cardiac research, and imaging of the mouse heart is challenging but crucial. In the present study we could show that adapting a common clinical MRI scanner is a feasible method to determine infarct size and functional data of mouse hearts *in vivo*.

## Abbreviations

|       |  |
|-------|--|
| MRI:  | Magnetic resonance imaging                           |
| CMR:  | Cardiac magnetic resonance imaging                   |
| I/R:  | Ischemia/reperfusion                                 |
| T:    | Tesla  |
| PSIR: | Phase-sensitive inversion recovery trueFISP sequence |
| TTC:  | Triphenyl tetrazolium chloride                       |
| FS:   | Fractional shortening                                |
| FAC:  | Fractional area change                               |
| LGE:  | Late gadolinium enhancement                          |
| ECG:  | Electrocardiography                                  |
| TR:   | Repetition time                                      |
| TE:   | Echo time  |
| TI:   | Inversion time.                                      |

## Conflict of Interest

The authors declare that they have no competing interests.

## Authors' Contributions

J. G. J. Voelkl conceived the study, and participated in its design and drafted the paper. B. J. Haubner participated in the design of the study. C. Kremser designed MRI protocol. A. Mayr analyzed the MRI data and helped interpret the data.

G. Klug analyzed MRI data and performed the statistical analysis. A. Loizides carried out imaging measurements. S. Müller designed echocardiographic measurement protocol. O. Pachinger helped to draft the paper. B. Metzler participated in study design and coordination and helped to draft the paper. All authors read and approved the final paper.

## Acknowledgments

This paper was supported by grants from the Austrian Society of Cardiology (Vienna, Austria) to B. Metzler and the Medizinische Forschungsfond Tirol to B. Metzler.

## References

- [1] P. Carmeliet and D. Collen, "Transgenic mouse models in angiogenesis and cardiovascular disease," *Journal of Pathology*, vol. 190, no. 3, pp. 387–405, 2000.
- [2] P. Balakumar, A. P. Singh, and M. Singh, "Rodent models of heart failure," *Journal of Pharmacological and Toxicological Methods*, vol. 56, no. 1, pp. 1–10, 2007.
- [3] J. N. Rottman, G. Ni, and M. Brown, "Echocardiographic evaluation of ventricular function in mice," *Echocardiography*, vol. 24, no. 1, pp. 83–89, 2007.
- [4] M. Nahrendorf, K.-H. Hiller, K. Hu, G. Ertl, A. Haase, and W. R. Bauer, "Cardiac magnetic resonance imaging in small animal models of human heart failure," *Medical Image Analysis*, vol. 7, no. 3, pp. 369–375, 2003.
- [5] F. H. Epstein, "MR in mouse models of cardiac disease," *NMR in Biomedicine*, vol. 20, no. 3, pp. 238–255, 2007.
- [6] C. Chapon, A. H. Herlihy, and K. K. Bhakoo, "Assessment of myocardial infarction in mice by late gadolinium enhancement MR imaging using an inversion recovery pulse sequence at 9.4T," *Journal of Cardiovascular Magnetic Resonance*, vol. 10, no. 1, article 6, 2008.
- [7] J. N. Oshinski, Z. Yang, J. R. Jones, J. F. Mata, and B. A. French, "Imaging time after Gd-DTPA injection is critical in using delayed enhancement to determine infarct size accurately with magnetic resonance imaging," *Circulation*, vol. 104, no. 23, pp. 2838–2842, 2001.
- [8] K. Klug, G. Gert, K. Thomas et al., "Murine atherosclerotic plaque imaging with the USPIO Ferumoxtran-10," *Frontiers in Bioscience*, vol. 14, pp. 2546–2552, 2009.
- [9] C. J. Berry, J. D. Miller, K. McGroary et al., "Biventricular adaptation to volume overload in mice with aortic regurgitation," *Journal of Cardiovascular Magnetic Resonance*, vol. 11, no. 1, p. 27, 2009.
- [10] T. Arai, T. Kofidis, J. W. M. Bulte et al., "Dual in vivo magnetic resonance evaluation of magnetically labeled mouse embryonic stem cells and cardiac function at 1.5 T," *Magnetic Resonance in Medicine*, vol. 55, no. 1, pp. 203–209, 2006.
- [11] W. D. Gilson and D. L. Kraitchman, "Cardiac magnetic resonance imaging in small rodents using clinical 1.5 T and 3.0 T scanners," *Methods*, vol. 43, no. 1, pp. 35–45, 2007.
- [12] F. Franco, S. K. Dubois, R. M. Peshock, and R. V. Shohet, "Magnetic resonance imaging accurately estimates LV mass in a transgenic mouse model of cardiac hypertrophy," *American Journal of Physiology*, vol. 274, no. 2, pp. H679–H683, 1998.
- [13] F. Franco, G. D. Thomas, B. Giroir et al., "Magnetic resonance imaging and invasive evaluation of development of heart failure in transgenic mice with myocardial expression of tumor necrosis factor- $\alpha$ ," *Circulation*, vol. 99, no. 3, pp. 448–454, 1999.
- [14] L. H. Michael, M. L. Entman, C. J. Hartley et al., "Myocardial ischemia and reperfusion: a murine model," *American Journal of Physiology*, vol. 269, no. 6, pp. H2147–H2154, 1995.
- [15] R. J. Kim, D. S. Fieno, T. B. Parrish et al., "Relationship of MRI delayed contrast enhancement to irreversible injury, infarct age, and contractile function," *Circulation*, vol. 100, no. 19, pp. 1992–2002, 1999.
- [16] B. Metzler, B. Haubner, E. Conci et al., "Myocardial ischaemia-reperfusion injury in haematopoietic cell-restricted  $\beta 1$  integrin knockout mice," *Experimental Physiology*, vol. 93, no. 7, pp. 825–833, 2008.
- [17] B. J. Haubner, G. G. Neely, J. G. J. Voelkl et al., "PI3K $\gamma$  protects from myocardial ischemia and reperfusion injury through a kinase-independent pathway," *PLoS ONE*, vol. 5, no. 2, article e9350, 2010.
- [18] B. Metzler, J. Mair, A. Lercher et al., "Mouse model of myocardial remodeling after ischemia: role of intercellular adhesion molecule-1," *Cardiovascular Research*, vol. 49, no. 2, pp. 399–407, 2001.
- [19] ImageJ software, <http://rsb.info.nih.gov/ij>.
- [20] D. M. Roth, J. S. Swaney, N. D. Dalton, E. A. Gilpin, and J. Ross Jr., "Impact of anesthesia on cardiac function during echocardiography in mice," *American Journal of Physiology*, vol. 282, no. 6, pp. H2134–H2140, 2002.
- [21] M. Siragusa, R. Katare, M. Meloni et al., "Involvement of phosphoinositide 3-kinase  $\gamma$  in angiogenesis and healing of experimental myocardial infarction in mice," *Circulation Research*, vol. 106, no. 4, pp. 757–768, 2010.
- [22] J. Weiss and F. Zimmermann, "Tribromoethanol (Avertin) as an anaesthetic in mice (multiple letters)," *Laboratory Animals*, vol. 33, no. 2, pp. 192–193, 1999.
- [23] W. Zeller, G. Meier, K. Bürki, and B. Panoussis, "Adverse effects of tribromoethanol as used in the production of transgenic mice," *Laboratory Animals*, vol. 32, no. 4, pp. 407–413, 1998.
- [24] C. Y. T. Hart, J. C. Burnett Jr., and M. M. Redfield, "Effects of avertin versus xylazine-ketamine anesthesia on cardiac function in normal mice," *American Journal of Physiology*, vol. 281, no. 5, pp. H1938–H1945, 2001.
- [25] G. Klug, T. Trieb, M. Schocke et al., "Quantification of regional functional improvement of infarcted myocardium after primary PTCA by contrast-enhanced magnetic resonance imaging," *Journal of Magnetic Resonance Imaging*, vol. 29, no. 2, pp. 298–304, 2009.
- [26] P. Kellman, A. E. Arai, E. R. McVeigh, and A. H. Aletras, "Phase-sensitive inversion recovery for detecting myocardial infarction using gadolinium-delayed hyperenhancement," *Magnetic Resonance in Medicine*, vol. 47, no. 2, pp. 372–383, 2002.
- [27] Z. Yang, S. S. Berr, W. D. Gilson, M.-C. Toufektsian, and B. A. French, "Simultaneous evaluation of infarct size and cardiac function in intact mice by contrast-enhanced cardiac magnetic resonance imaging reveals contractile dysfunction in noninfarcted regions early after myocardial infarction," *Circulation*, vol. 109, no. 9, pp. 1161–1167, 2004.
- [28] A. Mayr, J. Mair, M. Schocke et al., "Predictive value of NT-pro BNP after acute myocardial infarction: relation with acute and chronic infarct size and myocardial function," *International Journal of Cardiology*, 2009.

- [29] C. J. Berry, D. R. Thedens, K. A. Light-McGroary et al., “Effects of deep sedation or general anesthesia on cardiac function in mice undergoing cardiovascular magnetic resonance,” *Journal of Cardiovascular Magnetic Resonance*, vol. 11, no. 1, article 16, 2009.
- [30] F. Kober, I. Iltis, P. J. Cozzone, and M. Bernard, “Cine-MRI assessment of cardiac function in mice anesthetized with ketamine/xylazine and isoflurane,” *Magnetic Resonance Materials in Physics, Biology and Medicine*, vol. 17, no. 3–6, pp. 157–161, 2004.